Shape-Controlled Copper Selenide Nanocubes Synthesized by an Electrochemical Crystallization Method

ARTICLE *in* THE JOURNAL OF PHYSICAL CHEMISTRY C · JUNE 2009

Impact Factor: 4.77 · DOI: 10.1021/jp9025267

6 AUTHORS, INCLUDING:

Keju Sun
National Institute of Advanced Industrial S…
28 PUBLICATIONS **490** CITATIONS
SEE PROFILE

Zhaochi Feng
Chinese Academy of Sciences
151 PUBLICATIONS **4,798** CITATIONS
SEE PROFILE

Guanna Li
Technische Universiteit Eindhoven
23 PUBLICATIONS **211** CITATIONS
SEE PROFILE

Can Li
Guiyang university
503 PUBLICATIONS **15,334** CITATIONS
SEE PROFILE

THE JOURNAL OF PHYSICAL CHEMISTRY LETTERS

2009, *113,* 10833–10837
Published on Web 05/28/2009

Shape-Controlled Copper Selenide Nanocubes Synthesized by an Electrochemical Crystallization Method

Rui Yu,[†,‡] Tong Ren,[†] Keju Sun,[†,‡] Zhaochi Feng,[†] Guanna Li,[†,‡] and Can Li*[,†]

State Key Laboratory of Catalysis, Dalian Institute of Chemical Physics, Chinese Academy of Sciences, 457 Zhongshan Road, Dalian 116023, China, and Graduate University of Chinese Academy of Sciences, Beijing 100049, China

Received: March 20, 2009; Revised Manuscript Received: May 21, 2009

Nanocubes of copper selenide ($Cu_{2-x}Se$) have been synthesized through an electrochemical crystallization method using cetyltrimethylammonium bromide (CTAB) as the structure directing agent. The shapes of $Cu_{2-x}Se$ nanocubes can be controlled by the adsorption effect of CTA^+ hydrocarbon chain and Br^- ion on the facets of the $Cu_{2-x}Se$ crystals. First-principle quantum chemical calculations indicate that the preferential adsorption of bromide onto the {100} facets of $Cu_{2-x}Se$ crystals results in the final cubic shape. The ability to generate $Cu_{2-x}Se$ nanostructures with well-defined morphologies not only provides potential application of $Cu_{2-x}Se$ nanocubes in photoelectric devices but also provides a great opportunity to systematically study the relationship between their properties and geometric shapes.

Introduction

The synthesis of inorganic nanocrystals (NCs) with well-defined shapes has attracted much attention due to the strong correlation between the shapes and the properties, such as physical, chemical, electronic, optical, magnetic, and catalytic properties.[1] It has been well recognized that the preferential adsorption of molecules and ions onto different crystal faces could direct the growth of NCs into various shapes by controlling the growth rates along different crystal axes.[2] However, it is highly anticipated but still a challenge to synthetically control the shape of the nanoparticles due to the lack of knowledge on what capping agent or the combination of capping agents in synthesis solution would generate a desired shape and size of nanocrystal.[3] Many nanostructures such as nanorods, nanobelts, nanowires, nanorings, and other nanoconfigurations with interesting morphologies or specific structures have been successfully synthesized.[4] Nanocubes with wide applications have attracted special interest from both fundamental and applied aspects due to their shape dependent properties.[3,5] Many techniques have been developed to synthesize nanocubes including colloidal self-assemblies mode, hexadecyl trimethyl ammonium bromide-modified reaction, epitaxial electrodeposition, hydrothermal treatment, and so on.[6] For instance, Xia et al.[6,7] have done intensive research in the synthesis of nanocubes of noble metals. However, mainly metals nanocubes have been synthesized, and there is much less work on the semiconductor nanocubes. It is noteworthy that many fields would greatly benefit from the advances in the synthesis of well-defined nanostructures of semiconductors, including photonics, information storage, nanoelectronics, catalysis, and biosensors.[8] Therefore, it is a great interest but a challenge to develop a new synthetic method for the shape-controlled synthesis of semiconductor nanocubes.

We were motivated to study $Cu_{2-x}Se$ by its properties and potential applications as well as its unique crystal structures. $Cu_{2-x}Se$ is a well-known p-type semiconductor that has potential applications in solar cells, optical filter, superionic material, and thermoelectric converters.[9] $Cu_{2-x}Se$ possesses a direct band gap of 2.2 eV along with an indirect band gap of 1.4 eV for $x = 0.2$[10] and could be an excellent photon-electron conversion materials for both solar cells and photocatalysis. This material is also interesting because of the possibility of incorporating In to form the ternary material $CuInSe_2$[11] by incorporating indium into this binary compound. Therefore, many methods have been tried to synthesize $Cu_{2-x}Se$ micro- and nanocrystals with different morphologies, such as rods, spheres, platelets, nanowires, and nanocages.[12] Several reports on the electrodeposition of Cu−Se phase have been investigated.[13] However, to the best of our knowledge, there has been no report on the synthesis of single-crystalline $Cu_{2-x}Se$ nanocubes. Herein, we report a facile and shape-controlled synthesis of $Cu_{2-x}Se$ nanocubes, whose morphology can be synthetically controlled using the cationic surfactant cetyltrimethylammonium bromide (CTAB) as the morphology controlling agent.

The synthetical strategy included the cathodic electrodeposition of $Cu_{2-x}Se$ nanocubes from aqueous solution containing $CuSO_4$, H_2SeO_3, and CTAB at room temperature.

Figure 1a shows the X-ray diffraction (XRD) pattern of the sample deposited onto an ITO (indium tin oxide)-coated glass. The diffraction peaks at 26.6 and 44.2° are assigned to (111) and (220) planes of the cubic phase of $Cu_{2-x}Se$ ($F\bar{4}3m$, $a = 5.739$ Å, JCPDS Card No. 06-0680), while the peaks corresponding to (311) and (200) diffractions are not observed, indicating that $Cu_{2-x}Se$ crystals tend to be preferentially oriented parallel to the surface of the ITO substrate. Figure 1b,d shows the scanning electron microscope (SEM) results of the typical structure,

* To whom correspondence should be addressed. Telephone: +86-411-84379070. Fax: +86-411-84694447. E-mail: canli@dicp.ac.cn.
[†] Dalian Institute of Chemical Physics, Chinese Academy of Sciences.
[‡] Graduate University of Chinese Academy of Sciences.

10.1021/jp9025267 CCC: $40.75

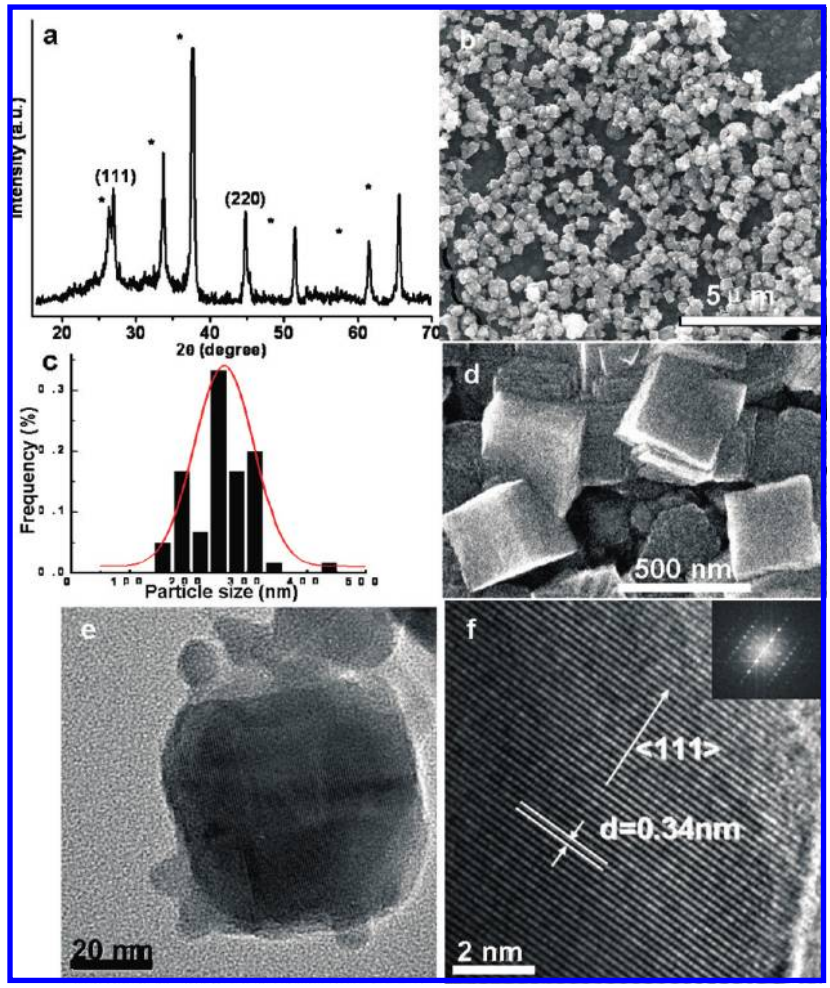

Figure 1. $Cu_{2-x}Se$ nanocubes electrodeposited at 65 °C using CTAB as surfactant. (a) Typical XRD pattern of $Cu_{2-x}Se$ crystals deposited on ITO substrate. Reflections generated by the ITO substrate are marked as *; (b,d) SEM images; (c) particle size distribution of the product $Cu_{2-x}Se$; (e) TEM image; and (f) HRTEM image (the inset is the corresponding FFT ED pattern).

indicating that the large quantity of $Cu_{2-x}Se$ with uniform morphology can be made using this approach. The yield of the $Cu_{2-x}Se$ nanocubes is estimated to be >80%, and the rest is the agglomeration of imperfect nanocubes. The average size of the nanocubes is about 250 nm (Figure 1c), with a standard deviation of 30−40%, suggesting that the size of the nanocubes is narrowly distributed. The x in $Cu_{2-x}Se$ is estimated to be 0−0.2 according to EDS analysis. The truncated shape of a single nanocube is clearly observed using transmission electron microscope (TEM, Figure 1e). High-resolution transmission electron microscope (HRTEM) image (Figure 1f) and the fast Fourier transform (FFT) pattern (Figure 1f, inset) reveal that the entire nanostructure is a cubic single crystal. The lattice fringes show an interlayer spacing of 0.34 nm, which are in good agreement with the lattice spacing of the (111) plane of cubic $Cu_{2-x}Se$ (d (111) = 0.333 nm for cubic $Cu_{2-x}Se$, JCPDS Card No. 06-0680).

To further confirm the formation of $Cu_{2-x}Se$ NCs on the ITO-coated glass surface, X-ray photoelectron spectra (XPS) was recorded with Al Kα radiation as the excitation source. The XPS spectrum of $Cu_{2-x}Se$ shows the presence of C, O, Cu, Se, and Sn components in full area of the sample (see the Supporting Information, Figure S1). Both the Cu $2p_{3/2}$ binding energy and Cu L_3VV kinetic energy are in agreement with the published results of monovalent copper.[13] The binding energy of Se $3d_{5/2}$ is 54.5 eV (Supporting Information, Figure S2c).

To the best of our knowledge, this is the first report that the $Cu_{2-x}Se$ nanocubes can be prepared by an electrochemical crystallization method. It is important to understand how the $Cu_{2-x}Se$ cubes were produced in the electrochemical way in the presence of CTAB. The SEM images in Figure 2a−e show the morphology evolution of $Cu_{2-x}Se$ as the concentration of CTAB increases. When no CTAB is present, thin films with truncated pyramid structures are obtained (as shown in Figure 2a). XRD pattern reveals that the product was Cu_3Se_2 ($P\bar{4}21m$, a = 6.403 Å, c = 4.277 Å, JCPDS Card No. 47-1745) (Figure 2f). When 0.001 M CTAB was introduced, the crystal phase is transformed into $Cu_{2-x}Se$ (as shown in Figure 2f), but the morphology is not obviously changed until the C_{CTAB} reaches 0.003 M. A dramatic transition from branched nanocubes, a mixture of branched and cubic ones, to purely cubic particles occurs with the CTAB concentration in the range of 0.003−0.008 M (Figure 2c−e), but the crystal phase remains to be $Cu_{2-x}Se$. In order to obtain well-defined shape as well as to explore the morphology control effect of other surfactants, we also tried SDS (sodium dodecylsulfonate), PVP (Polyvinylpyrrolidone), and Triton X-100, etc., but we have not observed the well controlled cubic morphology.

On the basis of the results presented above, the production of $Cu_{2-x}Se$ with nanocube morphology could be mainly attributed to the adsorption effect of CTAB. It is well known that CTAB is an effective surfactant, which consists of a hydrocarbon chain

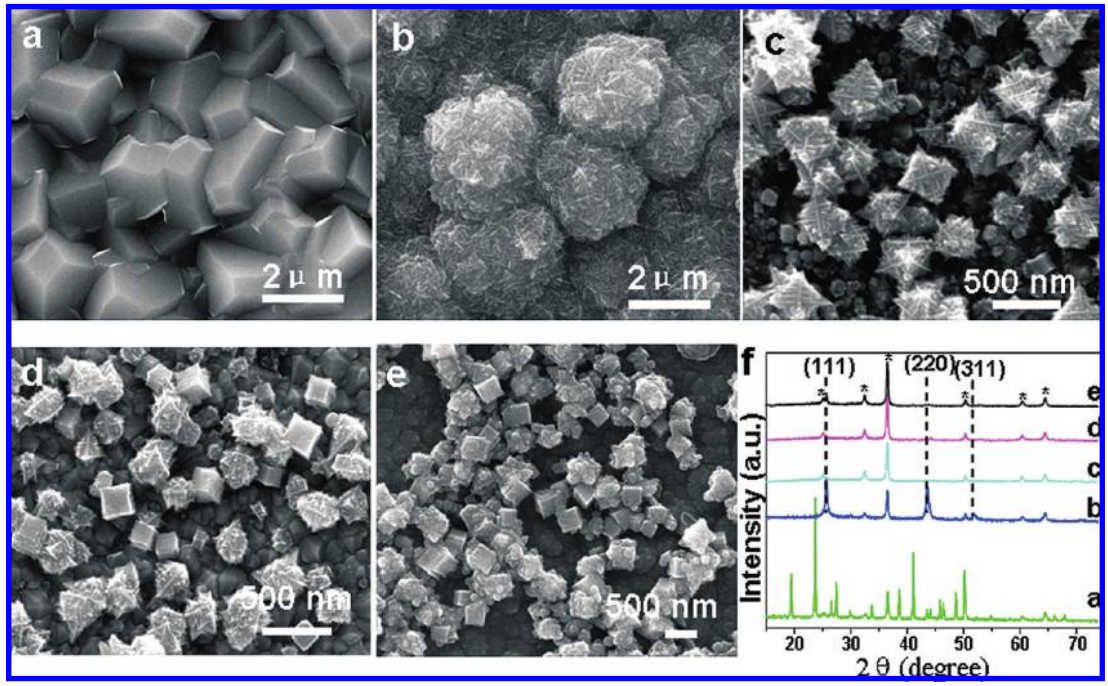

Figure 2. SEM images of $Cu_{2-x}Se$ nanoparticles prepared with different concentrations of CATB: (a) 0 mM, (b) 1 mM, (c) 3 mM, (d) 5 mM, (e) 8 mM; (f) the corresponding XRD patterns of panels a−e.

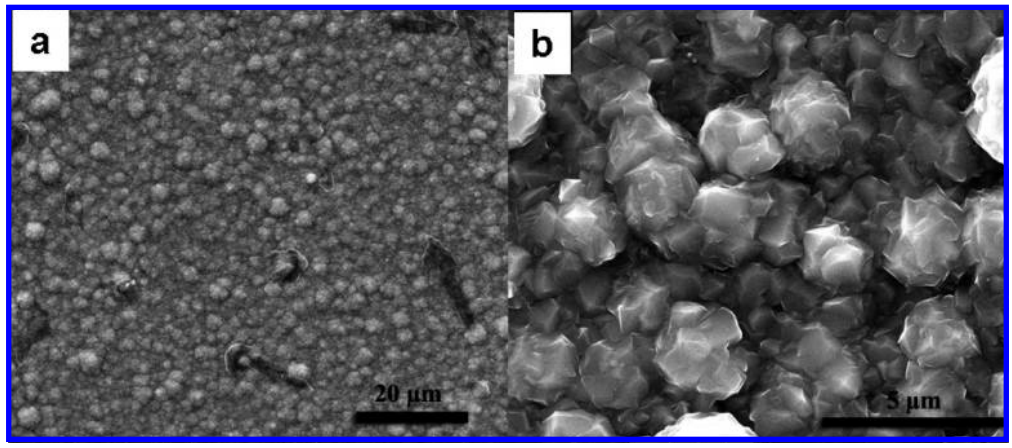

Figure 3. SEM images of (a) Cu_3Se_2 thin films synthesized with 0.008 M $CTA^+(HSO_4^-)$, (b) $Cu_{2-x}Se$ thin films synthesized with 0.008 M KBr.

(CTA^+) and a bromide ion (Br^-).[13] The adsorption of CTA^+ hydrocarbon chain on the surface of the particles inhibits the excess aggregation of copper selenides, thus offers a unique microenvironment for the formation of nanoparticles.[14] However, it is still unclear which ion can stabilize the {100} facets. In order to clarify the morphology formation mechanism, we investigated the adsorption effect of CTA^+ and Br^- on the phase transformation and morphology change of the copper selenides by replacing CTAB with $CTA^+(HSO_4^-)$ and KBr, respectively. When CTAB was replaced by $CTA^+(HSO_4^-)$, Cu_3Se_2 was formed in a thin film layer consisting of sphere clusters (Figure 3). When CTAB was replaced by KBr, the phase became $Cu_{2-x}Se$, but the structure is still in a layer of thin film with faceted crystals. The phase transformation is thus attributed to the presence of bromide ion while the morphology evolution, is controlled by the combination effect of CTA^+ hydrocarbon chain and the bromide ion. It could be assumed that Br^- ions act as the termination that prevents further deposition of Cu, Se species on the {100} factes of $Cu_{2-x}Se$.

When inorganic crystals are formed under equilibrium conditions, their crystal habit is determined by the relative order of surface energies.[15] The fastest crystal growth occurs in the direction perpendicular to the face with the highest surface energy, which results in the elimination of higher-energy surfaces while the lower-energy surfaces increase in area. When organic or inorganic additives are adsorbed on the surfaces during the crystal growth process, the relative order of surface energies could be modified.[5] Because of the anisotropy in adsorption stability, these additives adsorb on to a certain crystallographic plane more strongly than others. This preferential adsorption lowers the surface energy of the bound plane and hinders the crystal growth perpendicular to this plane, resulting in the controlled morphology.

To further validate the growth mechanism of $Cu_{2-x}Se$, we carried out theoretical calculations for $Cu_{2-x}Se$ formation with and without the Br-termination. Copper selenide $Cu_{2-x}Se$ is in the antifluorite structure and its space group is $F\bar{4}3m$[16] (Figure 4a). The face-centered matters usually tend to nucleate and grow into twinned and multiply twinned particles with their surfaces bounded by the lowest-energy {111} facets.[17] Therefore, the crystal shape of copper(I) selenide is determined by the relative growth rates of {100} and {111} faces. We thus investigate

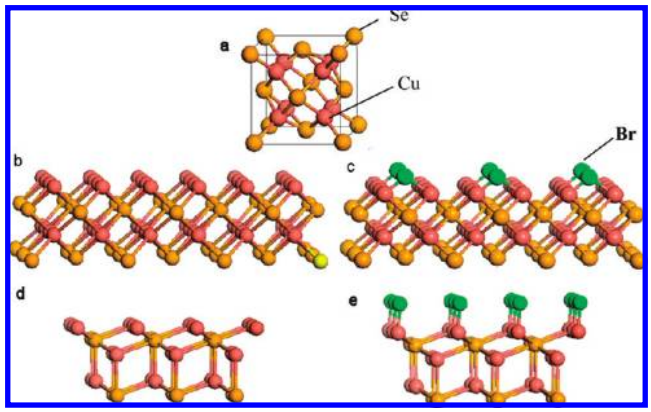

Figure 4. (a) Schematic description of the antifluorite structure of $Cu_{2-x}Se$; (b) atomic model of $Cu_{2-x}Se$ clean (100) surfaces; (c) (100) surfaces surrounded by adsorbate Br atom; (d) atomic model of $Cu_{2-x}Se$ clean (111) surfaces; (e) (111) surfaces surrounded by adsorbate Br atom. Cu, Se, and Br atoms are represented by pink, orange, and green spheres, respectively.

TABLE 1: Calculated Total Energies (eV) of the (111) and (100) Surfaces of $Cu_{2-x}Se$ under Clean Condition and Surrounded by Br Atom

	total energy (eV)		
surface	clean	Br-terminated	Br adsorption energy
(111)	−43.76	−45.60	−1.84
(100)	−42.15	−46.39	−4.24

the clean and Br^- terminated (111) and (100) surfaces using the first-principle calculation. Figure 4b−e illustrates the models of clean and Br-terminated (111) and (100) surfaces. The calculated total energies of the surfaces are listed in Table 1 from which two conclusions can be drawn: under the conditions without adsorption of any surfactant species, {111} facets are more stable than {100} facets, while for bromide-terminated surfaces, this relative stability is reversed; namely {100} facets are more stable than {111} facets. These results confirm that the preferential adsorption of Br^- ion onto {100} facets results in the cubic shape of $Cu_{2-x}Se$.

The morphology and dimensions of the product $Cu_{2-x}Se$ are also found to be dependent strongly on reaction conditions such as temperature, the concentration of $CuSO_4$ and H_2SeO_3, and the $CuSO_4/H_2SeO_3$ molar ratio. For example, when the temperature is lowered to 25 °C, the $Cu_{2-x}Se$ film with irregular shape is the major product. When the initial concentrations of $CuSO_4$ and H_2SeO_3 are decreased, for example, from 0.022 to 0.005 M for $CuSO_4$ and 0.016 to 0.004 M for H_2SeO_3 (as shown in Figure 5), the product is dominated by a platelike structure.

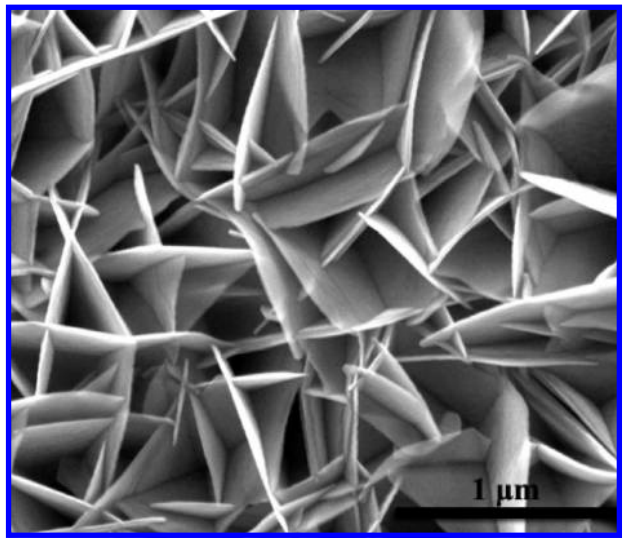

Figure 5. $Cu_{2-x}Se$ microplates synthesized with the concentration of Cu^{2+} 0.005 M and SeO_3^{2-} 0.003 M in the presence of 0.008 M CTAB.

In summary, we have successfully synthesized well-defined single-crystal $Cu_{2-x}Se$ nanocubes with an electrochemical crystallization method using CTAB as the capping agent. The formation of $Cu_{2-x}Se$ nanocubes is mainly owing to the adsorption effect of CTA^+ hydrocarbon chain and Br^- ion preferably adsorbed on the crystal surfaces of $Cu_{2-x}Se$. First-principle quantum chemical calculations indicate that the preferential adsorption of bromide onto {100} facets results in the final cubic shape. The $Cu_{2-x}Se$ nanocrystals with cubic shape are promising building blocks for many functional devices including solar cell, optics, and sensors.

Acknowledgment. This work was financially supported by the National Natural Science Foundation of China (20673112) and the Programme Strategic Scientific Alliances between China and The Netherlands (2008DFB50130).

Supporting Information Available: Descriptions of experimental details, synthetic, and characterization about the $Cu_{2-x}Se$ nanocubes. This material is available free of charge via the Internet at http://pubs.acs.org.

References and Notes

(1) (a) Alivisatos, A. P. *Science* **1996**, *271*, 933. (b) Sun, Y. G.; Xia, Y. N. *Science* **2002**, *298*, 2176. (c) Yan, H. Q.; He, R. R.; Pham, J.; Yang, P. D. *Adv. Mater.* **2003**, *15*, 402.

(2) (a) Puntes, V. F.; Krishnan, K. M.; Alivisatos, A. P. *Science* **2001**, *291*, 2115. (b) Filankembo, A.; Pileni, M. P. *J. Phys. Chem. B* **2000**, *104*, 5865. (c) Siegfried, M. J.; Choi, K. S. *Angew. Chem., Int. Ed.* **2008**, *47*, 368.

(3) Murphy, C. J. *Science* **2002**, *298*, 2139.

(4) (a) Wang, J.; Huang, H. C.; Kesapragada, S. V.; Gall, D. *Nano Lett.* **2005**, *5*, 2505. (b) Gao, P. X.; Ding, Y.; Mai, W.; Hughes, W. L.; Lao, C.; Wang, Z. L. *Science* **2005**, *309*, 1700. (c) Ding, Y.; Ma, C.; Wang, Z. L. *Adv. Mater.* **2004**, *16*, 1740.

(5) (a) Sherry, L. J.; Chang, S. H.; Schatz, G. C.; Van Duyne, R. P.; Wiley, B. J.; Xia, Y. N. *Nano Lett.* **2005**, *5*, 2034. (b) Sosa, I. O.; Noguez, C.; Barrera, R. G. *J. Phys. Chem. B* **2003**, *107*, 6269. (c) Siegfried, M. J.; Choi, K. S. *Adv. Mater.* **2004**, *16*, 1743.

(6) (a) Pileni, A.; Filankembo, M. P. *J. Phys. Chem. B* **2000**, *104*, 5865. (b) Yu, D. B.; Yam, V. W. W. *J. Am. Chem. Soc.* **2004**, *126*, 13200. (c) Xiong, Y. J.; Wiley, B.; Chen, J. Y.; Li, Z. Y.; Yin, Y. D.; Xia, Y. N. *Angew. Chem.* **2005**, *117*, 8127.

(7) (a) Xiong, Y. J.; Chen, J. Y.; Wiley, B.; Xia, Y. N.; Yin, Y. D.; Li, Z. Y. *Nano Lett.* **2005**, *5*, 1237. (b) Im, S. H.; Lee, Y. T.; Wiley, B.; Xia, Y. N. *Angew. Chem., Int. Ed.* **2005**, *44*, 2154. (c) Motiei, M.; Calderon-Moreno, J.; Gedanken, A. *Adv. Mater.* **2002**, *14*, 1169.

(8) (a) Robertson, J. *Mater. Sci. Eng., R* **2002**, *37*, 129. (b) Belomoin, G.; Therrien, J.; Smith, A.; Rao, S.; Twesten, R.; Chaieb, S.; Nayfeh, M. H.; Wagner, L.; Mitas, L. *Appl. Phys. Lett.* **2002**, *80*, 841. (c) Li, A. P.; Flack, F.; Lagally, M. G.; Chisholm, M. F.; Yoo, K.; Zhang, Z.; Weitering, H. H.; Wenderlken, J. F. *Phys. Rev. B* **2004**, *69*, 245.

(9) (a) Chen, W. S.; Stewart, J. M.; Mickelsen, R. A. *Appl. Phys. Lett.* **1985**, *46*, 1095. (b) Toyoji, H.; Hiroshi, Y. *Jpn. Kokai Tokkyo Koho* **1990**, *173*, 622. (c) Korzhuev, M. A. *Phys. Solid. State.* **1998**, *40*, 217. (d) Frangis, N.; Manolikas, C.; Amelinckx, S. *Phys. Status. Solidi. A* **1991**, *126*, 9. (e) Bhuse, V. M.; Hankare, P. P.; Garadkar, K. M.; Khomane, A. S. *Mater. Chem. Phys.* **2003**, *80*, 82.

(10) (a) Garcia, V. M.; Nair, P. K.; Nair, M. T. S. *J. Cryst. Growth* **1999**, *203*, 113. (b) Hermann, A. M.; Fabick, L. *J. Cryst. Growth* **1983**, *61*, 658. (c) Hamilton, M. A.; Barnes, A. C.; Beck, U.; Buchanan, P.; Howells, W. S. *J. Phys.: Condens. Matter* **2000**, *12*, 9525.

(11) (a) Contreras, M. A.; Egaas, B.; Ramanathan, K.; Hiltner, J.; Swartzlander, A.; Hasoon, F.; Noufi, R. *Prog. Photovoltaics* **1999**, *7*, 311. (b) Guillemoles, J. F.; Cowache, P.; Lusson, A.; Fezzaa, K.; Boisivon, F.; Vedel, J.; Lincot, D. *J. Appl. Phys.* **1996**, *79*, 7293.

(12) (a) Liu, Y. F.; Zeng, J. H.; Li, C.; Cao, J. B.; Wang, Y. Y.; Qian, Y. T. *Mater. Res. Bull.* **2002**, *37*, 2509. (b) Zhu, J. J.; Palchik, O.; Chen, S. G.; Gedanken, A. *J. Phys. Chem. B* **2000**, *104*, 7344. (c) Wang, W. Z.; Geng, Y.; Yan, P.; Liu, F. Y.; Xie, Y.; Qian, Y. T. *J. Am. Chem. Soc.* **1999**, *121*, 4062. (d) Hsu, Y. J.; Hung, C. M.; Lin, Y. F.; Liaw, B. J.; Lobana, T. S.; Lu, S. Y.; Liu, C. W. *Chem. Mater.* **2006**, *18*, 3323. (e) Cao, H. L.; Qian, X. F.; Zai, J. T.; Yin, J.; Zhu, Z. K. G. *Chem. Commun.* **2006**, 4548.

(13) (a) Dergacheva, M. B.; Chaikin, V. V.; Grigor'eva, V. P.; Pantileeva, E. P. *Russ. J. Appl. Chem.* **2004**, *77*, 1273. (b) Kemell, M.; Saloniemi, H.; Ritala, M.; Leskelä, M. *Electrochim. Acta* **2000**, *45*, 3737.

(14) Xie, Y.; Zheng, X. W.; Jiang, X. C.; Lu, J.; Zhu, L. Y. *Inorg. Chem.* **2002**, *41*, 387.

(15) Siegfried, M. J.; Choi, K. S. *Angew. Chem., Int. Ed.* **2005**, *44*, 3218.

(16) (a) Okada, Y.; Ohtani, T.; Yokota, Y.; Tachibana, Y.; Morishige, K. *J. Electron Microsc.* **2000**, *49*, 25. (b) Skomorokhov, A. N.; Trots, D. M.; Knapp, M.; Bickulova, N. N.; Fuess, H. *J. Alloy. Compd.* **2006**, *421*, 64. (c) Gladic, J.; Milat, O.; Vucic, Z.; Horvatic, V. *J. Solid State Chem.* **1991**, *91*, 213.

(17) Wang, Z. L. *J. Phys. Chem. B* **2000**, *104*, 1153.

JP9025267